A Theoretical Assessment of Factors Causing Different Molecular Volumes in Isotopologues

Ricard Gelabert,* Miquel Moreno, and José M. Lluch

Departament de Química, Universitat Autònoma de Barcelona, 08193 Bellaterra (Barcelona), Spain

Received: July 17, 2009; Revised Manuscript Received: September 28, 2009

A dynamical study has been performed to determine from first principles the molecular volume of C_6H_6 and C_6D_6 in the gas phase, starting from a normal-mode analysis and using anharmonic potential energy profiles at DFT level to determine vibrational eigenfunctions for all 30 degrees of freedom and using a Monte Carlo procedure to determine the appreciable ranges of variation of the coordinates of all atoms. The gas phase study reveals that the intrinsic volume of C_6D_6 is always the smallest, even though it increases faster with temperature than that of C_6H_6. In order to explain the experimentally observed fact that C_6D_6 volume is the largest at hight temperatures, the likely effect on molecular motions caused by the crystalline environment of a given molecule has to be considered.

1. Introduction

The behavior and properties of chemical systems are highly dependent on their electronic structure, which in turn is determined by the nuclear charges, the number of electrons, and the geometry of the molecule. Nuclear mass is the Cinderella in terms of strength of interaction with electrons and can only affect the behavior of the system when nuclear kinetic energy, that is, nuclear motion, is a differentiating aspect of the system.

Isotope effects are measurable changes observed in a system's behavior and/or properties when comparing isotopologues (two molecules differing only in the isotopic composition). In nature, the most extreme mass relation between isotopes is attained in the case of hydrogen: its heavier isotopes deuterium (D) and tritium (T) duplicate and triplicate its mass, respectively. Isotope effects due to H/D and H/T substitution are the most intense found in nature.[1]

By and large, the best known isotope effect is the kinetic isotope effect (KIE), which corresponds to the change in the phenomenological rate constant observed when certain atoms in the reactants are substituted by their isotopes. This finds an explanation in the differences in zero-point vibrational energy (ZPE) of the reactants and the transition state when considering different isotopologues and, especially in H/D and H/T isotopic substitution, the quantum mechanical tunneling effect. The intensity of these changes is maximal when the atoms affected by the changes are those that see their bonds formed or cleaved in the rate-determining step. Because of this and the extreme mass ratio for H/D substitution, H/D KIEs have been extensively used to elucidate reaction mechanisms.[1,2]

Isotope effects, however, do manifest themselves in many ways other than changes in reaction rates. It is nonetheless true that H/D and H/T substitution are still the cause of the strongest isotope effects in whatever way these manifest themselves. The relatively rich chemistry found in transition metal complexes that include hydrogen atoms in the coordination sphere of a metal has proved to be an especially rich area where isotope effects have been detected in unusual ways. For instance, measurable effects have been reported on the equilibrium constant of reactions involving transition metal complexes having hydrogen atoms directly coordinated to the metal.[3] Many marked isotope effects have been reported in transition metal polyhydride and dihydrogen complexes at spectroscopic level,[4] as well as on the geometry of systems. In the latter case, two specific families of compounds have been reported and characterized, whose properties—including geometry—are uniquely linked to the isotopic composition of the hydrogen ligands:[5] compresed dihydride[6−8] and elongated dihydrogen complexes.[9,10]

The rationale behind the dependence of geometry, or shape, of a molecule on isotopic composition is relatively simple. Focusing on the vibrational degrees of freedom of the molecule, vibrational motions occur normally over anharmonic potential energy profiles. Different isotopologues, because of their different mass, have different ZPEs and concomitantly the amplitude of the ground state vibrational eigenfunction is affected, being more spread out the higher the energy of the ground state. In general, in the ground state, heavier isotopologues should display a smaller amplitude of vibration.

On the basis of the changes that occur on the probability density of vibrational states, $|\psi_v|^2$, with isotopic substitution, measurable effects on *size* have been expected for some time, and even measured.[11,12] It has been known for a long time that deuterium has a smaller van der Waals radius than protium.[13] Given that van der Waals radii are interpreted in terms of the closest distance between nonbonded atoms before the onset of repulsion and because nuclear mass has a negligible effect on the electron cloud, this fact can only be understood in terms of deuterated isotopologues lying lower in vibrational energy and thus being more confined around the potential energy minimum than their protium isotopologues. Thus they are felt as "smaller".

When isotope effects are discussed, special care has to be taken with temperature dependence. Heavier isotopologues will have lower ZPE and consequently be more localized around the potential energy minimum. This would be true at $T = 0$ K. However, excited vibrational levels would be closer together in the heavier isotopologues and, thus, be populated faster on increasing temperature. Because excited states have also larger amplitude of vibration, this means that heavier isotopologues ought to see their effective size increase faster than their lighter counterparts, and in some special cases, the thermal effect could overcome the mass effect.

This issue was the target of an in-depth analysis published recently by Dunitz and Ibberson.[14] On the basis of the

* Corresponding author, ricard.gelabert@uab.cat.

10.1021/jp906766c
Published on Web 11/23/2009

elementary model of a harmonic oscillator to describe the essentials of molecular vibration, they estimated that for frequencies in the range of 100 cm^{-1} the vibrational amplitude of deuterium would be about 40% larger at 100 K than it was at 0 K, which is a very substantial increase. If low frequencies like this could be found in a system, it could be possible that at a certain temperature molecular volume of deuterium isotopologues were *larger* than those of their protium analogues. Such a system was found in solid benzene, where lattice modes of low frequency are present. On the basis of previous published results,[15] a precise experimental study was performed focusing on the temperature dependence of the unit cell volume (V_c) of solid C_6H_6 and C_6D_6 between practically 0 K and the melting point. It was found that molecular volume, taken as $V_c/4$ (being 4 the number of benzene molecules in the unit cell) was smaller for C_6D_6 at low temperatures but it increased faster and at about 170 K and up C_6D_6 was actually larger than C_6H_6.

Benzene, however, has no frequencies close to 100 cm^{-1} as an isolated molecule. These low frequencies can only be found in the solid phase, as lattice modes, that is, collective vibrations of two or more benzene molecules in the crystal. As such, the effective masses that move are at least those of C_6H_6 or C_6D_6 themselves. The ratio of masses between perdeutero- and perprotiobenzene is about 14:13, much smaller that that expected for deuterium and protium (2:1), so at first sight, differences in ZPE and in the energy spacing between vibrational levels should be very small, as should also be differences in the spreading of the vibrational eigenvectors. Thus, the thermal effect on molecular size should be similar for both isotopologues in the solid phase, and the reason for the larger slope observed for C_6D_6 on increasing temperature should be reanalyzed. Recently, the number of systems that show isotopic dependence on size or other properties related to crystalline structure has increased after reports of isotopically induced polymorphism in solid pyridine.[16]

This paper will try to give an explanation to the observed behavior of the molecular volume of perprotio- and perdeuterobenzene, based on a first principles approach. We will address a first-principles determination of gas phase volume of C_6H_6 or C_6D_6 (intrinsic volume) to explore their magnitude and how it changes with temperature, and the likely changes that occur when C_6H_6 or C_6D_6 are held captive in a crystal structure. The final goal is to discern which factors can lead to the experimental observed behavior.

2. Theory and Computational Methods

As stated, in this paper we are concerned with determining the molecular volumes of isotopologues of benzene both in the gas phase from first-principles and, more approximately, in the solid phase. The computational target is the volume of a C_6H_6 or C_6D_6 molecule, and this requires computing the average positions of each atom and their dispersions, considering correctly the effect of isotopic composition and temperature. The correct framework to tackle this task is a vibrational analysis. However, because the effects under scrutiny require careful consideration of quantum effects such as ZPE and also the penetration of the system in classically forbidden areas (tunneling), what is to be undertaken is a detailed quantum vibrational study of perprotio- and perdeuterobenzene.

2.1. Computing a Distribution of Cartesian Coordinates. The framework for this quantum vibrational study of the target systems is an anharmonic normal mode treatment (see Supporting Information for details). If the time-independent Schrödinger equation (TISE) of nuclear motion is separable in $3N - 6$ ordinary equations of the form

$$\left[-\frac{\hbar^2}{2}\frac{d^2}{dQ_i^2} + U^{(i)}(Q_i)\right]\chi^{(i)}(Q_i) = E^{(i)}\chi^{(i)}(Q_i) \quad (1)$$

then the global solution for the vibrational problem is

$$E_{\mathrm{vib},\mathbf{J}} = \sum_{i=1}^{3N-6} E_{j_i}^{(i)} \quad (2)$$

$$\chi_{\mathrm{vib},\mathbf{J}} = \prod_{i=1}^{3N-6} \chi_{j_i}^{(i)}(Q_i) \quad (3)$$

In the above equations, we use the collective index **J** to identify a global vibrational state of the molecule by specifying the vibrational states—ground or excited—of all normal modes: $\mathbf{J} = (j_1, j_2, ..., j_{3N-6})$. Finally, the final solution for the global nuclear problem would be of the form

$$\Gamma_{\mathrm{nuc}} = \chi_{\mathrm{trasl}}\chi_{\mathrm{rot}}\chi_{\mathrm{vib}} \quad (4)$$

where the Coriolis terms have been neglected altogether.

The information needed to determine the average position and dispersion in Cartesian coordinates for all nuclei is contained in the vibrational eigenvector χ_{vib}, However, χ_{vib} is expressed in normal mode coordinates. What is needed is a method to determine Cartesian coordinate dispersions from χ_{vib} that takes correctly into account temperature effects.

The probability density that, upon measurement of normal mode Q_i, its value is found to lie between Q_i and $Q_i + dQ_i$ is precisely $|\chi_{ji}^{(i)}(Q_i)|^2$, so it depends on the vibrational state j_i of normal mode i, be it ground or excited. Moreover, at a certain temperature T several excited states of the same mode might be populated to varying extents. To determine the expected values of Cartesian coordinates and their dispersion, a Monte Carlo method is proposed. We define a temperature-dependent normalized one-particle probability density function for each mode i as

$$\rho^{(i)}(Q_i, T) = \sum_{j_i=1}^{N_E} |\chi_{ji}^{(i)}(Q_i)|^2 \frac{e^{-E_{ji}^{(i)}/kT}}{Z^{(i)}(T)} \quad (5)$$

where Q_i is the ith normal mode coordinate (in principle $Q_i \in (-\infty,\infty)$) and $Z^{(i)}(T)$ is the vibrational canonical partition function for anharmonic normal mode i

$$Z^{(i)}(T) = \sum_{j_i=1}^{N_E} e^{-E_{ji}^{(i)}/kT} \quad (6)$$

In eqs 5 and 6 N_E is the number of vibrational eigenstates included in the computation, which should be large enough to guarantee that the partition function $Z^{(i)}(T)$ is numerically converged.

A given geometry of the molecule at temperature T can be obtained by selecting randomly the values of all normal mode coordinates $\mathbf{Q}_k$ based on their individual probability density functions (eq 5). This is done as follows: a $(3N - 6)$-tuple of random deviates $(\xi_1, \xi_2, ..., \xi_{3N-6})_k$ are sampled from a uniform distribution and are transformed into random deviates conforming to the individual probability density functions of each normal mode (eq 5) by means of the rejection method (also known as von Neumann method)[17] $(Q_1, Q_2, ..., Q_{3N-6})_k$, and stored on disk. This is done for a very large number of $(3N - 6)$-tuples, N_S, for each temperature studied. For the discussion at hand, let us call this set of N_S random structures in normal mode coordinates the population set at temperature T, $\mathbb{S}_T^{\mathrm{nm}}$. Following the procedure described, structures in $\mathbb{S}_T^{\mathrm{nm}}$ appear in the set according to a distribution that takes into account: (1) correct individual

vibrational probability densities (derived from correct anharmonic one-dimensional quantum dynamics calculations, see below) and (2) the correct populations of excited states, after a Boltzmann distribution within each normal mode. The studies of atomic positions must proceed from analysis of the members in $\mathbb{S}_T^{\mathrm{nm}}$.

To determine the dispersion of the position of a given atom at temperature T, the full set $\mathbb{S}_T^{\mathrm{nm}}$ is transformed into Cartesian coordinates. If $\mathbf{Q}_k \in \mathbb{S}_T^{\mathrm{nm}}$ then the *augmented* normal mode vector $\mathbf{Q}_k^{\mathrm{tr}}$ is defined as

$$\mathbf{Q}_k^{\mathrm{tr}} = (\mathbf{Q}_k,0,0,0,0,0,0) \tag{7}$$

where the six-zero vector refers to overall *t*ranslation and *r*otation. So, $\mathbf{Q}_k^{\mathrm{tr}}$ are $3N$-component vectors. Then a set of Cartesian structures $\mathbb{S}_T^{\mathrm{Cart}}$ is obtained as (see eqs S3 and S8 in the Supporting Information)

$$\mathbf{x}_k = \mathbf{x_0} + \mathbf{M}^{-1/2}\mathbf{L}\mathbf{Q}_k^{\mathrm{tr}} \quad x_k \in \mathbb{S}_T^{\mathrm{Cart}} \tag{8}$$

where $\mathbf{x_0}$ is the Born−Oppenheimer (BO) minimum.

Analysis of the thermal position and dispersion of coordinate ζ (any Cartesian coordinate of an atom in the molecule), the building blocks of the coming discussions on molecular volume in section 3, is done as follows. A normalized frequency histogram $N_T(\zeta)$ is computed to determine the density of structures in $\mathbb{S}_T^{\mathrm{Cart}}$ that have a certain value for ζ. We define the *maximum appreciable value* of ζ (ζ^+), as the value of ζ below which a certain fraction σ of structures in $\mathbb{S}_T^{\mathrm{Cart}}$ have been found

$$\int_{\zeta_{\min}}^{\zeta^+(T)} N_T(\zeta)\,\mathrm{d}\zeta = \sigma \tag{9}$$

Likewise, we define the *minimum appreciable value* of ζ (ζ^-), as the value of ζ below which a fraction $1 - \sigma$ of structures in $\mathbb{S}_T^{\mathrm{Cart}}$ have been found

$$\int_{\zeta_{\min}}^{\zeta^-(T)} N_T(\zeta)\,\mathrm{d}\zeta = 1 - \sigma \tag{10}$$

where $\zeta_{\min}$ is the smallest value ever found for ζ in $\mathbb{S}_T^{\mathrm{Cart}}$. Equations 9 and 10 are solved for ζ^+ and ζ^- for each value of T. We mention here that $\zeta^+(T) - \zeta^-(T)$ can be considered the appreciable range of thermal variation of coordinate ζ at temperature T: in random measurements of ζ at temperature T the probability of finding a value of $\zeta \in [\zeta^-, \zeta^+]$ is $2\sigma - 1$. For instance, in the calculations that follow $\sigma = 0.95$: this means that the ranges of variation of all Cartesian coordinates considered encompass 90% of the samples.

The parameters in the calculations that follow are $\sigma = 0.95$, $N_S = 10^5$.

The above procedure to obtain estimate ranges for the coordinates of different atoms at different temperatures can only be achieved if the eigenvalues and eigenvectors of the vibrational Hamiltonian (eq 1) are known, and this requires us to know the potential energy along all given normal mode ($U^{(i)}$, eq S12 in Supporting Information). Thus, we detail here the steps to determine the normal modes, determining the individual potential energy profiles and solving the TISE for vibration, in this order.

2.2. Determination of Normal Modes and Vibrational Frequencies. To determine the normal mode coordinates, energetic information on the topography of the BO potential energy surface is needed. This information has been obtained from first-principles calculations through use of electronic structure quantum chemistry software. The Gaussian 03 program has been used for all calculations.[18] Electronic structure calculations have been done at the Density Functional Theory (DFT) level.[19] The functional chosen for the electronic structure calculation has been the three-parameter hybrid functional of Becke, and the Lee, Yang, and Parr correlation functional (B3LYP).[20,21] The valence triple-ζ 6-311++G(d,p) basis set has been selected for all calculations.[22,23] Even though normal modes depend on isotopic composition, geometry of stationary points on the BO potential energy surface does not. Determination of the geometry of the potential energy minimum of benzene ($\mathbf{x}_0$) has been carried out in the D_{6h} symmetry group by minimization of the energy. The structure was reoriented along the principal axes of inertia and subsequently, the Cartesian second derivative matrix $\mathbf{H}$ has been computed through analytical second derivatives and stored. Afterward, the mass-weighted Hessian matrix $\tilde{\mathbf{H}}$ (Eq S5, see Supporting Information) has been computed and diagonalized to render the eigenvectors (normal modes, Eq S7, see Supporting Information). This has been done independently for C_6H_6 and C_6D_6, as normal modes depend on mass.

2.3. Solving the Vibrational Problem. A linear path in mass-weighted coordinates has been determined for each normal mode i, given paremeterically as a function of a scalar parameter λ

$$\mathbf{F}^{(j)}(\lambda) = \pm\lambda\mathbf{Q}_j \tag{11}$$

where, because each $\mathbf{Q}^{(i)}$ has been normalized to unit length, λ has the meaning of mass-weighted distance traversed along mode i on a linear path. Several structures in each path have been prepared by varying λ from zero to some possitive value. For C_6H_6 each path was determined with 21 structures, while in the case of C_6D_6, owing to its larger mass, a total of 29 structures were prepared for each path. In each case, the maximum values of $|\lambda|$ were scaled such that lower frequency normal modes were projected further to make sure that the linear path was computed from far enough to guarantee that many bound vibrational states could be computed accurately.

All structures thus obtained were transformed back into full $3N$ Cartesian space through use of eqs 7 (replacing $\mathbf{Q}_k$ with $\mathbf{F}^{(i)}$) and 8, and then single point electronic structure calculations were carried out on all of them. The resulting ground-state electronic energies were fitted into a cubic splines functional form.[17] These functions are the individual normal mode potential energy profiles $U^{(i)}$ in eq 1, and we highlight here that they are not quadratic forms: anharmonicity within each normal mode has been explicitly considered. For each isotopologue, the $3N - 6$ one-dimensional TISEs (eq 1) have been solved to obtain vibrational eigenvectors and eigenvalues. To achieve this, after determining the one-dimensional potential energy profiles along each normal mode $\{U^{(i)}\}_{i=1-3N-6}$, the matrix representation of the Hamiltonian operator for each normal mode has been constructed using the discrete variable representation (DVR) of Colbert and Miller.[24] Eigenvalues and eigenvectors have been found through diagonalization of this matrix. The number of points used to represent the nuclear Hamiltonian operator has been of 100 points, which means that in theory up to 100 one-particle vibrational eigenstates and eigenvectors have been obtained. The number of states actually considered in the calculations (N_E in eqs 5 and 6) has been different in each mode and isotopologue, taking always the last state that lied below the smallest of the two boundary energies. At any rate, N_E never went below 25 states (that is the case of the highest frequency mode of C_6H_6). The additional points included in all calculations have contributed to give a more converged result and a more detailed knowledge of the shape of the vibrational eigenfunctions.

3. Results and Discussion

In order to discuss from a theoretical point of view the factors that influence molecular volume in crystalline benzene, it is

necessary to analyze the experimental data available from which the current discussion springs. C_6H_6 and C_6D_6 crystals are orthorhombic and belong to space group *Pbca*, with a total of four molecules in the unit cell.[25−27] The actual data accessible to experiment is the unit cell volume (V_c) and discussion on molecular volume has been done assuming that $V_{mol} = V_c/4$.[14] This approach is reasonable but caution has to be used in interpreting the data. Molecular volume can be conceived as the space strictly used by the molecule and so unavailable to other molecules in the surroundings; more graphically, it would be the volume of a continuous (i.e., infinitely divissible), uniform, and uncompressible fluid displaced due to immersion of the target molecule in it. It is then clear that $V_c/4$ and V_{mol} do not match, especially when considering representation of the unit cell (see refs 14, 15, and 27). The reason lies in the unavoidable amount of interstitial space to be found in the unit cell. This space is already present in compact packing, such as face-centered cubic, and is foreseeably much larger in the case of molecular crystals.

In view of the above, the most desirable approach would be to determine theoretically the parameters of the unit cell directly using theoretical methods. In this regard, DFT methods for periodic (crystal) systems have become invaluable aids in research of solid phase problems. Of course, such a study should be followed by an in-depth vibrational analysis, like that proposed in section 2, to determine the effects on V_c of isotopic substitution and temperature, with the natural alterations due to the number of atoms. There are two main obstacles in this approach that make it especially difficult. First, even though computational software aimed at the electronic structure of solids based on DFT is available, calculations are expensive, and because the unit cell includes four molecules, the number of potential energy profiles $U^{(i)}$ is much larger and each of their points much more expensive in computer resources, making this calculation really onerous. Second, determination of unit cell parameters through optimization of molecular crystals is troublesome in DFT, because long-range dispersive interactions (dispersion forces) cannot be incorporated onto a theory based on one-electron density approximation exchange-correlation functionals, like LDA or GGA DFT.[28] Moreover, as the reported difference[14] at 0 K for V_c is of just 2.080 Å^3, this shortcoming of current DFT methods compromises their capability to capture such a subtle effect in the solid phase. While this paper was being written, much progress has been done in this regard by using techniques based on the adiabatic connection fluctuation−dissipation theorem within the random phase approximation.[29]

Taking into account the above considerations, we have decided to avoid computation of the unit cell directly. The observed changes in unit cell volume must be rooted in intrinsic volume changes of C_6H_6 and C_6D_6. Thus, an accurate estimation of a single molecule's volume in the gas phase from a theoretical point of view and taking into account all factors (masses, anharmonicity and temperature) ought to provide piercing insights into the issue of molecular volume. This approach can only establish tendencies and cannot reproduce the experimental values reported for the unit cell volume, because solid phase effects are missing and interstitial space is not accounted for.

To obtain the theoretical estimate of the volume of a C_6H_6/C_6D_6 molecule, information on the positions of the constituent nuclei as a function of temperature and isotopic constitution has to be obtained. To this end, the procedure based on normal-mode analysis put forth in section 2 has been followed. The study starts off by determining the ground state structure of the minimum in the BO potential energy surface (structure $\mathbf{x_0}$). This

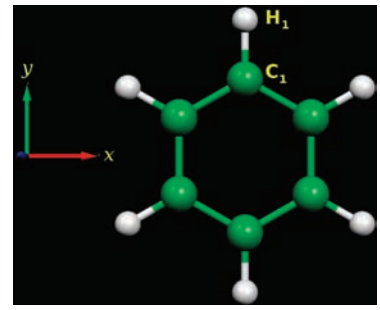

Figure 1. Structure of the BO potential energy minimum of benzene. Coordinate origin is the center of mass of the benzene molecule, but axes have been drawn shifted to the left for clarity. The structure is contained in the *xy* plane. Positive *z* values lie between the figure and the reader. In the text, carbon and hydrogen atoms are labeled $C_1\cdots C_6$ and $H_1\cdots H_6$. Only the first atom of each kind is labeled in the figure; the rest are numbered in ordered sequence clockwise from the first.

minimum energy structure has D_{6h} symmetry, and at the level of calculation used, the geometry (bond distances) is r_{C-C} =1.395 Å and r_{C-H} = 1.084 Å. In principle, these distances could be compared to experimentally determined values. However, and this is especially relevant in this study, the geometrical values of r_{C-C} and r_{C-H} shown above describe only the geometry of the minimum energy structure on the BO potential energy surface and therefore lack consideration of nuclear motion, so small deviations between geometries derived from BO PES minima and experimental data are to be expected and not attributable to experimental error, except if anharmonicity is absent from the system in the lowest lying vibrational states.

The structure obtained has been reoriented so that the principal axes of inertia coincide with the regular Cartesian axes. Figure 1 shows the structure and, especially important for the discussion that will follow, the orientation with respect to Cartesian axes and numbering of atoms.

The Hessian of the minimum energy structure has been determined. The mass-weighted Hessians for C_6H_6 and C_6D_6 have been computed and diagonalized to render the eigenvalues and eigenvectors (normal modes). With the eigenvalues the harmonic frequencies (eq S9 in Supporting Information) have been obtained. Benzene has 30 vibrational modes. In the case of C_6H_6 their harmonic frequencies lie between 3193 and 409 cm^{-1}, while for C_6D_6 they are between 2368 and 355 cm^{-1}. The Supporting Information analyzes the contribution to H(D) atom motion of each of these harmonic normal modes.

Effects on individual normal modes translate differently on individual atoms' coordinates. To determine the observable effects on the thermal spread of coordinate values of constituent atoms, the procedure set forth in Section 2.1 has been followed. A total of $N_S = 10^5$ samples per normal mode per isotopologue and per temperature have been determined to generate the normal mode set $\mathbb{S}_T^{nm}$ at each temperature. Next the Cartesian set $\mathbb{S}_T^{Cart}$ has been obtained through use of eqs 7 and 8. To analyze the results, we have determined the maximum and minimum appreciable values of the atomic coordinates (eqs 9 and 10) with $\sigma = 0.95$: This means that ζ^+ represents the value of the Cartesian coordinate below which 95% of the samples are to be found, and ζ^- represents the value of the same coordinate below which only 5% of the samples are to be found. Thus, the range $[\zeta^-, \zeta^+]$ encompasses 90% of the samples. This approach allows determination of the probable ranges of variation of each individual Cartesian coordinate and later, to estimate molecular volume. Higher values of σ yield unstable

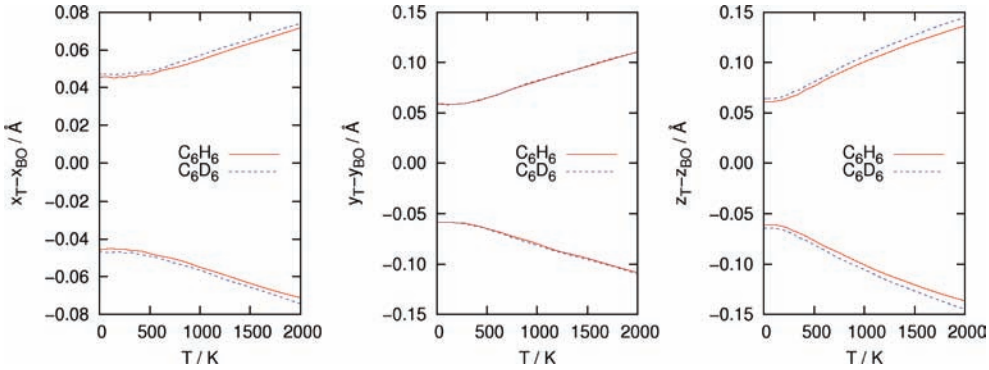

Figure 2. Ranges of variation on x (left), y (middle), and z (right) Cartesian coordinates of atom C_1, as derived from the Monte Carlo procedure discussed in the text, for the C_6H_6 (red) and C_6D_6 (blue) isotopologues as a function of temperature. The values are given relative to the value of the coordinate at the BO potential energy minimum. Note the different range shown for the x coordinate (left).

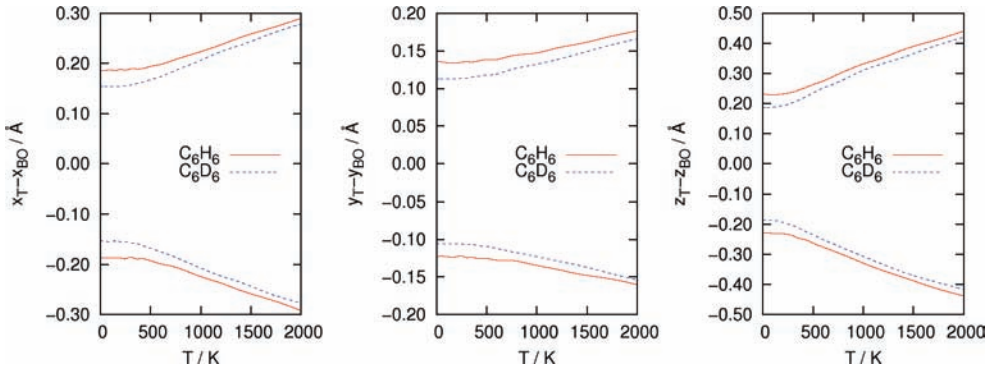

Figure 3. Ranges of variation on x (left), y (middle), and z (right) Cartesian coordinates of atom H_1, as derived from the Monte Carlo procedure discussed in the text, for the C_6H_6 (red) and C_6D_6 (blue) isotopologues as a function of temperature. The values are given relative to the value of the coordinate at the BO potential energy minimum. Note the different ranges covered in the ordinate axis in the three panels.

values for ζ^+ and ζ^- because of statistical noise in the set and would require an even larger sampling space (N_S). Figure 2 displays the ranges of variation of the position of carbon atoms, while Figure 3 does the same for hydrogen and deuterium atoms.

We begin the discussion on the effect of isotopic composition and temperature on the carbon atoms of benzene. As seen in Figure 2, a remarkable fact is that changes in the H/D composition of benzene do have an effect on the expected positions of carbon atoms (similar to a "secondary isotope effect"). This is explainable because normal mode coordinates depend on mass, and hence a change in mass affects the *direction* of all normal modes, however slightly. Especially on the range of the z Cartesian coordinate, the effect of H/D substitution is to increase the spread: the carbon ring is somewhat larger in deuterated benzene than in perprotiobenzene.

Quite naturally the effects of H/D substitution are more noticeable on the expected position and spread of H/D atoms themselves, as seen in Figure 3. Protium atoms have a larger dispersion in all directions than deuterium ones. However, as shown in Figure 3 and for all coordinates, distance between appreciable values of all coordinates for C_6H_6 and C_6D_6 gets closer as temperature increases. This means that the appreciable values of all coordinates for C_6D_6 increase faster with temperature than their C_6H_6 counterparts. This is caused, of course, by a smaller spacing between vibrational energy levels in the heavier isotopologue, which get populated at lower T.

The general effects in terms of atomic coordinates and their dispersions are already clear in Figures 2 and 3. Nevertheless, it is worth producing a single figure representing the estimate within our approach of the single molecule volume of C_6H_6 and C_6D_6 as a function of temperature, in the understanding that V_{mol} cannot coincide, because of the reasons brought up at the beginning of section 3, with those reported from experiment. This actually means deciding for a model shape and to compute its volume. This is not really simple, as molecular (or atomic) volume is an ill-defined quantity, as much as atomic radii are. In good approximation, benzene molecules can be modeled as far as shape is concerned, as oblate ellipsoids.[14] If a is the shorter semiaxis and b any of the long ones in such a form, then the volume is simply

$$V_{mol} = \frac{4\pi}{3} ab^2 \tag{12}$$

All that remains is to estimate a and b from $\mathbb{S}_T^{Cart}$.

However, one needs to bear in mind that the maximum and minimum appreciable values of all Cartesian coordinates so far computed refer to *nuclei*. To determine the molecular volume, it is compulsory to account for the effect of the electron cloud, which in fact prevents other atoms or molecules from moving closer thanks to electron−electron repulsion, which is what "occupied volume" is all about. The concept of closest approach between atoms due to the size of their electron clouds is what lies at the heart of van der Waals radii. Originally van der Waals radii were compiled by Bondi[30] from a variety of data sources; despite this heterogeneous origin, they have withstood the test of time, being used routinely in a plethora of applications. Current consensus is that they are reasonable figures. van der Waals radii of H and C, constituent atoms of our system, are 1.20 and 1.70 Å, respectively, but we note that other authors have suggested slightly different values for H.[31] We point the interested reader to a recent work by Truhlar and co-workers that revisits the van der Waals radii and evaluates them for elements of the main group via sophisticated ab initio methods,

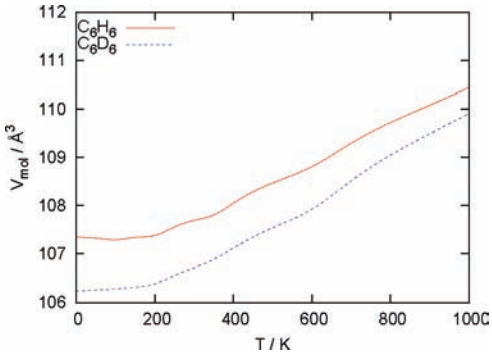

Figure 4. Molecular volume of gas-phase C_6H_6 and C_6D_6, computed assuming an oblate ellipsoid shape with semiaxes given by eq 13 and 14. Maximum and minimum appreciable values of Cartesian coordinates have been computed at $\sigma = 0.95$, which is equivalent to 90% probability.

achieving a consistent set, even though the values for C and H remain unaltered.[32]

We can now define quantitatively the values for a and b considering the outermost limits achieved by the nuclei (with $\sigma = 0.95$) and the van der Waals radius of the affected atoms. Thus, considering benzene molecules to be oblate ellipsoids (eq 12) a is the shortest semiaxis and should correspond to one-half the thickness along the z axis of the molecule in the center of the ring. Assuming that we can accept this thickness is majoritarily provided by carbon atoms, we propose

$$a \equiv \frac{1}{2}(z^{+}_{C_1} - z^{-}_{C_1}) + r_W(C) \tag{13}$$

For b, we consider that the outermost in-plane distance ever achieved by any atom is described by

$$b \equiv \frac{1}{2}(y^{+}_{H_1} - y^{-}_{H_4}) + r_W(H) \tag{14}$$

where the coordinates of C_1, H_1, and H_4 have been taken just for convenience, and could, with proper modifications of the formulas, be substituted by those of other atoms of the same type. We have taken Bondi's van der Waals radii of H and C, and the maximum and minimum appreciable values of the Cartesian coordinates have been computed to include 90% of probability within. Results are depicted in Figure 4.

As $T \rightarrow 0$ K Figure 4 shows that, as expected, C_6D_6 is noticeably smaller than C_6H_6. The predicted difference at 0 K is about 1 Å^3. In absolute terms this difference is about twice as large as in the experimental case (0.52 Å^3),[14] which taking into account the complexity of the procedure used is a remarkable agreement. As a side note, we remark that the $T =$ 0 K volume for C_6H_6 and C_6D_6 is reasonably close to the values experimentally found in the solid phase of 115.886 and 115.366 Å^3, respectively, which as mentioned before do include interstitial space. As T increases, the molecular volumes of both isotopologues increase but at different rates: C_6D_6 does so faster than C_6H_6, so the molecular volume difference decreases upon increasing T, again in agreement to what is reported from experiment. This is due to the fact that vibrational levels of C_6D_6 are populated faster because they are closer in energy than those of the lighter isotopologue. However, in our gas phase calculations there is no crossing between the curves of the two molecular volumes, contrary to what happens in experiments with solid phase.

The reasons for this apparent failure of our model to reproduce such a crossover temperature are to be found of course in the energetic position of vibrational levels. As a matter of fact, the energetic position of excited vibrational levels determines how easily these get populated as T increases. A look at our results shows that for C_6H_6 molecular volume increases 0.35 Å^3 in going from 0 to 300 K, while the gross experimental increase over the equivalent range is close to 11 Å^3 (for C_6D_6, the theoretical volume increase over the 0−300 K range is 0.48 Å^3, and the experimental value is approximately 13 Å^3).[14] It seems that to reproduce the experimental increase of molecular volume, a denser packing of vibrational states is needed. Indeed, Dunitz and Ibberson, while elaborating on their qualitative harmonic oscillator model, concluded that to observe such a crossover temperature frequencies around 100 cm^{-1} are needed. As mentioned before, however, our gas-phase calculations of benzene have rendered a lowest frequency mode of 409 cm^{-1} (355 cm^{-1}) for C_6H_6 (C_6D_6); see Figure S1 in the Supporting Information.

We believe that the difference in behavior is due to differences characteristic of the solid phase. A gas-phase molecule of N atoms has $3N - 6$ vibrational degrees of freedom, plus three global traslations and three global rotations. However, when forming a crystal of M such molecules, the number of global rotations and traslations of the crystal remains 6, which renders a much larger number of internal vibrations at $3MN - 6$. When the vibrational degrees of freedom of the crystal and the constituent individual molecules are compared, a large number of collective motions have appeared as a result of the loss of the six rotational and traslational modes of each molecule. These are called lattice modes. Being collective motions of two or more molecules in the crystal, the masses involved are large and frequencies are very low. The hypothesis raised by Dunitz and Ibberson is possible only in the solid phase of this molecular crystal. However, the mass difference between C_6H_6 and C_6D_6 is very small (the mass ratio is about 13:14), which makes it unclear that it might have appreciable effects, such as overcoming the tendencies of molecular volume in the gas phase and induce a crossover temperature in which C_6D_6 molecules were actually larger than its lighter counterpart.

As explained before, applying the same accurate approach that we have used for the gas phase in the solid phase is unaffordable, as it would require at the very least computing in the same way potential energy profiles for all modes (molecular or lattice) that arise in the unit cell, and even that would not include lattice modes that involve molecules from more than a unit cell. Moreover, current DFT methods are inaccurate because of the known problems with long-range dispersive interactions. Instead, we have chosen to estimate the kind of changes that set on when a benzene molecule, whose intrinsic molecular volume temperature dependence we have accurately determined, finds itself in an environment like that of the crystal. While this will rule out quantitative agreement, we believe that it suffices to establish the nature (and direction) of the changes induced by the solid phase.

An important difference between gas and solid phase is that traslation (and rotation) of a single molecule is no longer free in the solid. The approximate method that we adopt here is to quantify the extent to which the center of mass (CM) of a given benzene molecule is able to move, taking into account the influence of neighboring molecules in an approximate way and, especially, considering the effect that temperature has on the population of CM motion states. Because gas-phase results obtained so far denote atomic motion relative to CM, combining both thermal motions in an appropriate way might provide a reasonable estimate of how molecular volume gets affected when in the solid phase.

In our simplified model to represent this solid phase, each benzene molecule can move in the lattice in three directions. In this model we focus solely on the CM dynamics and disregard rotations. We write, then

$$\Gamma_{nuc} = \chi_{trasl}\chi_{rot}\chi_{vib} \sim \chi_{CM}\chi_{vib} \quad (15)$$

where χ_{CM} describes the in-lattice traslational motion of a benzene molecule (or more properly, its periodic motion within the lattice, so a global vibration). To determine it, a TISE has to be solved

$$\left[-\frac{\hbar^2}{2m}\nabla_{CM}{}^2 + V_{CM}\right]\chi_{CM} = E_{CM}\chi_{CM} \quad (16)$$

In this approximate model we express the above equation in Cartesian coordinates of the CM, and assuming that the potential can be written as $V_{CM}(\mathbf{R}_{CM}) = V^x_{CM}(x_{CM}) + V^y_{CM}(y_{CM}) + V^z_{CM}(z_{CM})$. This lets us write eq 16 as three ordinary differential equations of the form

$$\left[-\frac{\hbar^2}{2m}\frac{d^2}{d\zeta_{CM}{}^2} + V^\zeta_{CM}(\zeta_{CM})\right]\chi_{CM}(\zeta_{CM}) = E^\zeta_{CM}\chi_{CM}(\zeta_{CM}) \quad (17)$$

where $\zeta_{CM} = x_{CM}, y_{CM}, z_{CM}$.

What kind of potential energy function is V^ζ_{CM}? Ideally we should determine V^ζ_{CM} from potential energy calculations in the solid phase, by quantifying the effects on potential energy of variations on the position of a target C_6H_6 molecule with respect to its neighbors. Because of DFT deficiences and the onerous costs involved in such a calculation, we have not considered a quantitative determination of the interactions (potential energy) in the solid phase due to displacements of a benzene molecule from its equilibrium position in the crystal, opting instead for an affordable approximation to determine the energy levels open to the motion of the CM of a given benzene molecule. It is clear that it should have a minimum at the value of ζ_{CM} where the stable geometry of the cell is to be found. Displacing the CM from this equilibrium position means approaching another benzene molecule and going away from another along the ζ axis; this motion should bring up the potential energy as the balance of dispersive interactions with the closest neighbors in the lattice is disrupted (otherwise, there would not be a minimum of crystal potential energy and hence, also not a recognizable crystal structure). Finally, displacements beyond a certain distance should bring rapid increase of potential energy, as then steric contact of the displaced molecule with the closest neighbor sets on. The following function meets these requirements

$$V^\zeta_{CM}(\zeta_{CM}) = \begin{cases} \frac{1}{2}k\zeta^2_{CM} & -\frac{L}{2} \le \zeta_{CM} \le \frac{L}{2} \\ \infty & |\zeta_{CM}| > \frac{L}{2} \end{cases} \quad (18)$$

that is, a symmetrical harmonic oscillator centered at the origin which jumps up to infinity when displacements from the equilibrium position exceed $(L)/2$ in any direction, this representing the gross distance to the closest molecule. In a recent paper, Kearley et al. have published a combined experimental and theoretical study of the lattice dynamics and molecular vibrations of crystalline C_6H_6 and C_6D_6.[28] Among the wealth of data published there is a comprehensive list of vibrational frequencies of both isotopologues and their assignment at the Γ point. There is a large number of modes between 50 and 127 cm^{-1}, labeled as lattice modes. For our needs we have taken the lowest lattice mode reported (55 cm^{-1} for C_6H_6 and 50 cm^{-1} for C_6D_6), as the source to determine k for each isotopologue through

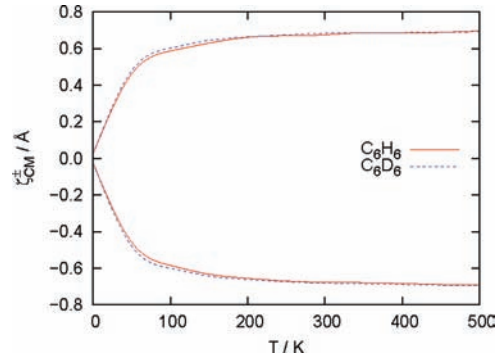

Figure 5. Appreciable displacements of a Cartesian coordinate of the center of mass, ζ^+_{CM} and ζ^-_{CM}, as derived from the Monte Carlo procedure discussed in the text, for the C_6H_6 (red) and C_6D_6 (blue) isotopologues as a function of temperature. For a given isotopologue (color) ζ^+_{CM} is the upper curve, while ζ^-_{CM} is the lower one. ζ is any Cartesian coordinate of the center of mass.

$$\nu = \frac{1}{2\pi}\sqrt{\frac{k}{m}} \quad (19)$$

where m is the mass of the vibrating particle, here taken as the mass of C_6H_6 and C_6D_6. As for L, we have taken a value of $3a_0$, which represents in practice that the limits of motion within the lattice of a given benzene molecule are going to be ± 0.79 Å away from the equilibrium position. Taking into account the bulk of the benzene molecule, this value has been considered reasonable. We mention here that we have assumed that the three Cartesian directions of the CM motion have been assigned the same force constant k and box length L (eq 18). Thus the CM moves within a cubic box of hard walls.

Mimicking now the procedure followed for the internal motion in benzene shown in the first part of this paper, we have solved eq 17 using the DVR method and determined wave functions and energy levels for the CM motion. Using the same procedure as before, we have produced for each temperature the minimum and maximum appreciable values of ζ_{CM}, ζ^-_{CM} and ζ^+_{CM}, respectively, corresponding to a fraction of structures with $\sigma = 0.95$. Figure 5 shows the temperature dependence of the appreciable displacements along a Cartesian coordinate of the center of mass. As a matter of fact, a surprising feature comes up in Figure 5, which is that the appreciable range of variation of the CM coordinates (difference between the top and bottom curves in Figure 5) are slightly larger for C_6D_6 than for C_6H_6. This behavior is especially visible at low temperatures and persists with vanishingly small differences for higher values of T, where the value for both isotopologues tends asymptotically to the same value of ± 0.79 Å. The volume traversed by the CM in our model can easily be computed from these data, assuming that the behavior along the other Cartesian coordinates is the same, from

$$V_{CM} = (\zeta^+_{CM} - \zeta^-_{CM})^3 \quad (20)$$

and is depicted in Figure 6

Let us analyze the behavior observed for V_{CM}. At low temperatures the value tends to almost zero. Even for the small frequencies here considered, the ground state wave function is largely localized around the equilibrium position ($\zeta_{CM} = 0$), which explains the small value of V_{CM} (of the order of 10^{-4} $Å^3$). Because of the small values of the frequencies, the vibrational energy spacing is also very small—approximately

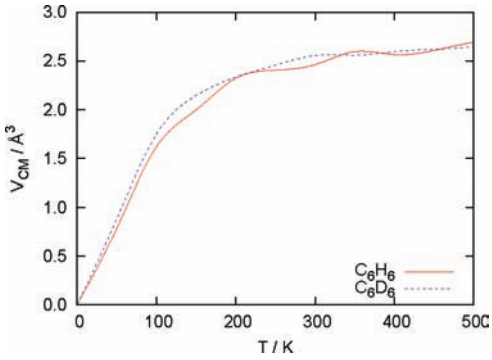

Figure 6. Volume traversed by the center of mass, assuming that all three Cartesian degrees of freedom are equivalent, for the C_6H_6 (red) and C_6D_6 (blue) isotopologues as a function of temperature. The small amplitude oscillations observed in the figure at high temperature are due to statistical noise in the sample.

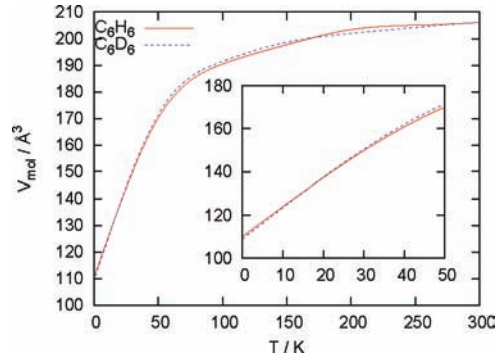

Figure 7. Estimate of the molecular volume as a function of temperature when vibrational motion of the center of mass is considered, for the C_6H_6 (red) and C_6D_6 (blue) isotopologues. The inset displays an enlargement of the 0−50 K temperature range, to show the crossing of the two curves at ∼20 K.

0.16 kcal mol^{-1} for C_6H_6 and 0.14 kcal mol^{-1} for C_6D_6—even at very low temperatures there is an important population in excited states: This is the reason for the steep increase observed in V_{CM} up to 100 K. Afterward, the increase slows down markedly and shows signs of reaching an asymptotic limit at ∼3 Å^3. The states being populated at ∼100 K are no longer harmonic: the fronts of the wave function are approaching the $\pm L/2$ hard limits and the system can better be described now as a particle-in-a-box than a harmonic oscillator. In this case, the vibrational motion of the CM is no longer governed by the effects of dispersion forces, but rather by the steric interactions that arise from collisions with neighboring molecules in the crystal, and this change of regime looks reasonable. Should the behavior of this vibrational motion be classical, at high T the CM would be moving freely inside a cubic space of side length L, so V_{CM} ∼4 Å^3. As seen in Figure 6, at temperatures on the order of 500 K the system is still somewhat far from this value, the reason coming from the quantum condition that forces the wave function to be continuous—and hence, zero—at $\zeta_{CM} = \pm L/2$.

Summarizing: C_6D_6 might be intrinsically smaller but it moves more freely in the crystal than C_6H_6 does at low temperatures.

Including traslational motion of the CM can change the *perception* of the molecular volume of benzene in the crystal, as now the maximum extent to which a certain atom moves should also include the additive motion of the CM. In our simple model the three Cartesian directions have been ascribed the same energetic description. Thus, still considering as valid the oblate ellipsoid shape, the thickness of the ellipsoid can be seen now as

$$a \equiv \frac{1}{2}[(z^+_{C_1} + z^+_{CM}) - (z^-_{C_1} + z^-_{CM})] + r_W(C) \qquad (21)$$

and the width

$$b \equiv \frac{1}{2}[(y^+_{H_1} + y^+_{CM}) - (y^-_{C_4} + y^-_{CM})] + r_W(H) \qquad (22)$$

With the new definitions of the a and b semiaxes, molecular volumes including an estimation of volume due to vibrational motion of the CM is straightforward to compute and is represented in Figure 7. It is very remarkable that, even with such strong approximations as have been considered to represent the effect of the solid phase on molecular volume estimates, the behavior of both isotopologues has changed. Now the temperature dependence is much more pronounced: in the range from 0 to 300 K C_6H_6 has had an increase of molecular volume of ∼96 Å^3 and C_6D_6 of ∼97 Å^3. These values exceed what is observed experimentally by about an order of magnitude (it must be borne in mind that *before* considering the effect of CM motion, the increase of volume over the same range was underestimated by almost 2 orders of magnitude, though). More remarkably, while at $T \rightarrow 0$ K C_6H_6 is still the largest isotopologue, there is a certain temperature now at which both molecular volumes become equal (∼20 K), and at higher temperatures C_6D_6 becomes the largest isotopologue. This can only be because of the changes induced by considering vibrational motion of the CM in the crystal, and the lack of quantitative agreement with experiment can be attributed to the extreme simplicity of the model used.

A consideration in this regard comes from the fact that we have used the smallest frequencies reported by Kearley et al.[28] Because of this, the localization of excited-state vibrational wave functions corresponding to the motion of the CM is smaller than it would be in the case of frequencies around 100 cm^{-1}. Use of higher frequencies for the lattice would cause a larger localization around $\zeta_{CM} = 0$ for excited states, and thus, the temperature-induced dispersion (Figure 5) would be more damped, as would also be the volume traversed by the center of mass (Figure 6). This would limit to some extent the exaggerated growth of molecular volume shown in Figure 7. This reduced protagonism of the contribution to molecular volume coming from motion of the center of mass would also likely delay the temperature at which C_6D_6 becomes the largest isotopologue to a higher value.

How is it that including to some extent the characteristics of the solid phase changes the volume dependence in the right direction? We think that our treatment of gas-phase volume for benzene is quite accurate, and about the only debatable point is actually whether the oblate ellipsoid shape is a good decision to estimate the molecular volume. As noted before, molecular volume is an ill-defined quantity and besides the data coming from experimental sources are not corrected to exclude interstitial spaces that are unavoidable in the solid phase, anyway. The figures produced for molecular volume in the gas phase and its temperature dependence are very reasonable in our case: The heavier isotopologue is the smallest at 0 K, and the thermal dilatation of the heavier isotopologue is the largest, in accordance with expectations. The fact that molecular volume of C_6D_6 does fail to become the largest at a given temperature is understood as none of its natural harmonic frequencies goes under the threshold of 100 cm^{-1} proposed by Dunitz and Ibberson.[14]

What about the solid phase, then? If C_6D_6 is the smallest in the gas phase, the intrinsic space it uses in the crystal should also be the smallest at any temperature. However, crystal structure is the outcome of the balance of all interactions at molecular level of the constituent molecules, and as such is a function of electronic structure, which at large determines which are the positions of all nuclei and molecules that bring the potential energy of the crystal to a minimum. These interactions depend solely on the nuclear charges and number of electrons, so they are not expected to be different among isotopologues. In this way, we can imagine crystals of C_6H_6 and C_6D_6 to be essentially identical as far as positions of the nuclei are being discussed. Given however that vibrational motion makes C_6D_6 slightly smaller, a periodic packing of C_6D_6 molecules leaves more *empty space* in between once vibrational motion is considered than a C_6H_6 crystal. Thus, even though C_6D_6 molecules are smaller, each individual C_6D_6 molecule has more room to move, and moves further than the equivalent C_6H_6 molecules. Then, upon increasing temperature C_6D_6 occupies this larger interstitial space faster than C_6H_6. This causes the perceived volume of C_6D_6 in the solid phase to be eventually the largest at high temperatures.

Conclusions

A study has been carried out to determine the intrinsic molecular volume of C_6H_6 and C_6D_6 in the gas phase, starting from a normal-mode analysis and using anharmonic potential energy profiles at DFT level to determine vibrational eigenfunctions for all 30 vibrational degrees of freedom, using a Monte Carlo based method to obtain appreciable ranges of variation of all Cartesian coordinates for all atoms. As a result, intrinsic volume of C_6D_6 in the gas phase is always smaller than that of C_6H_6, even though it increases faster with temperature. It fails, however, to become larger, as reported to happen from experimental studies in the solid phase.[14]

To consider somehow the effect of low-frequency lattice modes present in the crystal, a similar procedure has been set up to simulate global motion of the center of mass in the lattice subject to dispersive forces caused by neighboring molecules in the crystal in an approximate way. The result of this approximate study reveals an increased rate of growth of molecular volume than in the gas phase and, more significantly, the appearance of a temperature at which molecular volume is larger for C_6D_6 than for C_6H_6. In quantitative terms this is precisely what has been observed experimentally. The results are interpreted in terms of a larger ease of motion of the heavier isotopologue due to the reduced size of all molecules in the crystal with respect to those of C_6H_6 and a mostly invariant crystal structure.

Acknowledgment. The authors are grateful for financial support from the "Ministerio de Ciencia e Innovación" (project CTQ2008-02403/BQU) and from the "Generalitat de Catalunya" (project 2009SGR409).

Supporting Information Available: Derivation of the anharmonic normal mode coordinates, analysis of light atom motion in the harmonic normal modes of C_6H_6 and C_6D_6, list of anharmonic frequencies, and details on the random number generator used. This material is available free of charge via the Internet at http://pubs.acs.org.

References and Notes

(1) *Isotope Effects in Chemistry and Biology*; Kohen, A., Limbach, H.-H., Eds.; CRC Press, Taylor & Francis Group: Boca Raton, FL, 2006.
(2) Cleland, W. W. *J. Biol. Chem.* **2003**, *278*, 51975–51984.
(3) Torres, L.; Gelabert, R.; Moreno, M.; Lluch, J. M. *J. Phys. Chem. A* **2000**, *104*, 7898–7905.
(4) Gelabert, R.; Moreno, M.; Lluch, J. M. *Ber. Bunsen-Ges. Phys. Chem.* **1998**, *102*, 354–358.
(5) Morris, R. H. *Coord. Chem. Rev.* **2008**, *252*, 2381–2394.
(6) Gelabert, R.; Moreno, M.; Lluch, J. M.; Lledós, A.; Heinekey, D. M. *J. Am. Chem. Soc.* **2005**, *127*, 5632–5640.
(7) Gelabert, R.; Moreno, M.; Lluch, J. M. *Chem.—Eur. J.* **2005**, *11*, 6315–6325.
(8) Schloerer, N.; Pons, V.; Gusev, D. G.; Heinekey, D. M. *Organometallics* **2006**, *25*, 3481–3485.
(9) Gelabert, R.; Moreno, M.; Lluch, J. M.; Lledós, A. *J. Am. Chem. Soc.* **1997**, *119*, 9840–9847.
(10) Gelabert, R.; Moreno, M.; Lluch, J. M.; Lledós, A. *J. Am. Chem. Soc.* **1998**, *120*, 8168–8176.
(11) Mislow, K.; Wahl, G. H.; Gordon, A. J.; Graeve, R. *J. Am. Chem. Soc.* **1963**, *85*, 1199–1199.
(12) Felder, T.; Schalley, C. A. *Angew. Chem., Int. Ed.* **2003**, *42*, 2258–2260.
(13) Ubbelohde, A. R. *Trans. Faraday Soc.* **1936**, *32*, 525–529.
(14) Dunitz, J. D.; Ibberson, R. M. *Angew. Chem., Int. Ed.* **2008**, *47*, 4208–4210.
(15) Bürgi, H. B.; Capelli, S. C.; Goeta, A. E.; Howard, J. A. K.; Spackman, M. A.; Yufit, D. S. *Chem.—Eur. J.* **2002**, *8*, 3512–3521.
(16) Crawford, S.; Kirchner, M. T.; Bläser, D.; Boese, R.; David, W. I. F.; Dawson, A.; Gehrke, A.; Ibberson, R. M.; Marshall, W. G.; Parsons, S.; Yamamuro, O. *Angew. Chem., Int. Ed.* **2009**, *48*, 755–757.
(17) Press, W. H.; Flannery, B. P.; Teukolsky, S. A.; Vetterling, W. T. *Numerical Recipes in Fortran*, 2nd ed.; Cambridge University Press: Cambridge, U.K., 1992.
(18) Frisch, M. J.; Trucks, G. W.; Schlegel, H. B.; Scuseria, G. E.; Robb, M. A.; Cheeseman, J. R.; Montgomery, J. A., Jr.; Vreven, T.; Kudin, K. N.; Burant, J. C.; Millam, J. M.; Iyengar, S. S.; Tomasi, J.; Barone, V.; Mennucci, B.; Cossi, M.; Scalmani, G.; Rega, N.; Petersson, G. A.; Nakatsuji, H.; Hada, M.; Ehara, M.; Toyota, K.; Fukuda, R.; Hasegawa, J.; Ishida, M.; Nakajima, T.; Honda, Y.; Kitao, O.; Nakai, H.; Klene, M.; Li, X.; Knox, J. E.; Hratchian, H. P.; Cross, J. B.; Bakken, V.; Adamo, C.; Jaramillo, J.; Gomperts, R.; Stratmann, R. E.; Yazyev, O.; Austin, A. J.; Cammi, R.; Pomelli, C.; Ochterski, J. W.; Ayala, P. Y.; Morokuma, K.; Voth, G. A.; Salvador, P.; Dannenberg, J. J.; Zakrzewski, V. G.; Dapprich, S.; Daniels, A. D.; Strain, M. C.; Farkas, O.; Malick, D. K.; Rabuck, A. D.; Raghavachari, K.; Foresman, J. B.; Ortiz, J. V.; Cui, Q.; Baboul, A. G.; Clifford, S.; Cioslowski, J.; Stefanov, B. B.; Liu, G.; Liashenko, A.; Piskorz, P.; Komaromi, I.; Martin, R. L.; Fox, D. J.; Keith, T.; Al-Laham, M. A.; Peng, C. Y.; Nanayakkara, A.; Challacombe, M.; Gill, P. M. W.; Johnson, B.; Chen, W.; Wong, M. W.; Gonzalez, C.; Pople, J. A. *Gaussian 03, Revision C.02*; Gaussian, Inc.: Wallingford, CT, 2004.
(19) Parr, R. G.; Yang, W. *Density Functional Theory of Atoms and Molecules*; Oxford University Press: Oxford, U.K., 1989.
(20) Lee, C. T.; Yang, W. T.; Parr, R. G. *Phys. Rev. B* **1988**, *37*, 785–789.
(21) Becke, A. D. *J. Chem. Phys.* **1993**, *98*, 5648–5652.
(22) Krishnan, R.; Binkley, J. S.; Seeger, R.; Pople, J. A. *J. Chem. Phys.* **1980**, *72*, 650–654.
(23) Clark, T.; Chandrasekhar, J.; Spitznagel, G. W.; Schleyer, P. V. *J. Comput. Chem.* **1983**, *4*, 294–301.
(24) Colbert, D. T.; Miller, W. H. *J. Chem. Phys.* **1992**, *96*, 1982–1991.
(25) Bacon, G. E.; Curry, N. A.; Wilson, S. A. *Proc. R. Soc. London, Ser. A* **1964**, *279*, 98–110.
(26) Jeffrey, G. A.; Ruble, J. R.; McMullan, R. K.; Pople, J. A. *Proc. R. Soc. London, Ser. A* **1987**, *414*, 47–57.
(27) David, W. I. F.; Ibberson, R. M.; Jeffrey, G. A.; Ruble, J. R. *Physica B* **1992**, *180*, 597–600.
(28) Kearley, G. J.; Johnson, M. R.; Tomkinson, J. *J. Chem. Phys.* **2006**, *124*, 044514.
(29) Lu, D. Y.; Li, Y.; Rocca, D.; Galli, G. *Phys. Rev. Lett.* **2009**, *102*, 206411.
(30) Bondi, A. *J. Phys. Chem.* **1964**, *68*, 441.
(31) Rowland, R. S.; Taylor, R. *J. Phys. Chem.* **1996**, *100*, 7384–7391.
(32) Mantina, M.; Chamberlin, A. C.; Valero, R.; Cramer, C. J.; Truhlar, D. G. *J. Phys. Chem. A* **2009**, *113*, 5806–5812.

JP906766C